PROGRESS IN PHOTOVOLTAICS: RESEARCH AND APPLICATIONS
Prog. Photovolt: Res. Appl. 2003; **11**:225–230 (DOI: 10.1002/pip.494)

Research

SHORT COMMUNICATION: ACCELERATED PUBLICATION

Properties of 19·2% Efficiency ZnO/CdS/CuInGaSe$_2$ Thin-film Solar Cells‡

Kannan Ramanathan*,†, Miguel A. Contreras, Craig L. Perkins, Sally Asher, Falah S. Hasoon, James Keane, David Young, Manuel Romero, Wyatt Metzger, Rommel Noufi, James Ward and Anna Duda

National Renewable Energy Laboratory, 1617 Cole Boulevard, Golden, CO 80401, USA

We report the growth and characterization of record-efficiency ZnO/CdS/CuInGaSe$_2$ thin-film solar cells. Conversion efficiencies exceeding 19% have been achieved for the first time, and this result indicates that the 20% goal is within reach. Details of the experimental procedures are provided, and material and device characterization data are presented. Published in 2003 by John Wiley & Sons, Ltd.

KEY WORDS: copper indium gallium selenide; Cu(In,Ga)Se$_2$; ternary chalcopyrite; thin film solar cells; three stage process; photovoltaics; solar conversion efficiency

INTRODUCTION

Achieving higher conversion efficiencies in thin-film solar cells and modules is an important goal for the Photovoltaic (PV) Program funded by the US Department of Energy. The maturity and viability of a technology is measured by the progress made in the efficiencies of small-area cells made in research laboratories, mini-modules made in pilot production, and finally, the large-area modules produced by the manufacturer. The conversion efficiency of solar cells fabricated in research laboratories represent a useful reference point in this journey. At the National Renewable Energy Laboratory (NREL), we have been using the three-stage process to fabricate the highest-efficiency CuInGaSe$_2$ (CIGS) thin-film solar cells. Although this represents a specialized case of preparing the absorbers by co-evaporation, the process allows for careful compositional control and the ability to vary the bandgap gradients within the absorber.

Improvements made to the growth of the CIGS absorbers by the three-stage process resulted in an 18·8% efficient device in 1999.[1] The above paper also discussed the specifics of the growth, the potential impact of preferred orientation, and the optimization of window layers. We have also demonstrated that high-efficiency devices can be fabricated in a routine manner[2] and highlighted the importance of electronic effects at the interfaces during the formation of CdS/CIGS structures.[3] The present paper attempts to document the various properties of the recent record-efficiency CIGS cells and to identify the potential causes that contribute to the increase in efficiency. This is not always an easy task because one is attempting to explain what caused small, but significant, increases over the solar cell parameters measured in a previous best cell. However, a summary of the properties of the absorbers and devices, and identification of any unique properties or features can pave the way for more careful and controlled experimentation, and testing of key ideas.

* Correspondence to: Kannan Ramanathan, NREL, 1617 Cole Boulevard, Golden, Co 80401, USA.
† E-mail: kannan_ramanathan@nrel.gov

Contract/grant sponsor: USDOE PV Program; contract/grant number: DE-AC36-99GO 10337.

Received 28 February 2003
Revised 29 March 2003

EXPERIMENTAL DETAILS

The procedures for fabricating CIGS absorbers by the three-stage process have been reported previously.[1] CIGS absorbers were grown on soda-lime glass substrates with a sputter-deposited Mo layer. Compositional control was achieved by detecting the temperature change of the substrate during the Cu-poor to Cu-rich transition at the end of the second stage. The third stage consists of the evaporation of In and Ga in the presence of Se. CdS deposition was performed with a solution consisting of 0·0015 M $CdSO_4$, 1·5 M NH_4OH, and 0·0075 M thiourea. The samples were immersed in the bath at room temperature and the temperature of the bath was increased to 60°C. CdS thin films in the thickness range of 50–60 nm were deposited in 16 min. The ZnO layer was deposited in two stages. A 90-nm-thick undoped layer was first deposited from a pure ZnO target using Ar/O_2 working gas, and a second layer of about 120 nm was deposited from an Al_2O_3-doped ZnO target. The sheet resistance of the bilayer was about 65–70 Ω/square. Sputtering the undoped layer in oxygen ambient ensures high transmission and resistivity. Ni/Al grids were deposited by electron beam evaporation. The cell area was defined by photolithographic procedures and by etching the ZnO and CdS. The total area of the cells was 0·408 cm^2. A 100-nm-thick MgF_2 film was deposited to serve as an anti-reflection coating. Current–voltage characteristics of the devices were measured under AM 1·5 global spectrum for 1000 W/m^2 irradiance.

RESULTS AND DISCUSSION

The co-evaporation system used in this work allows us to deposit absorber layers on 7·5 × 7·5 cm substrates. The location of the evaporation sources results in a gradient in the In and Ga compositions from one end of the sample to the other. The Cu source is placed between the In and Ga sources, and the distribution of Cu varies across the substrate. The end point of the second stage is determined by sensing the drop in temperature of the substrate, and it is measured by a thermocouple resting on the rear side of the substrate.[4] At this point, the semiconductor film is a two-phase mixture of the chalcopyrite CIGS and Cu_xSe, and the latter can segregate at the surface as a liquid phase. The third stage is terminated when the value of the thermocouple reading reaches the original value before the film became two-phase in the second stage. Using this approach, we have fabricated high-efficiency devices with high open-circuit voltages and fill factors.

Figure 1 shows the current–voltage (J–V) characteristics of the 19·2% efficiency solar cell measured under the standardized AM 1·5 global spectrum, and Table I lists the photovoltaic cell parameters of three cells measured. The bandgap of the absorber estimated from quantum efficiency curves is 1·12 eV. When compared with the previous record cell with the same bandgap, the open-circuit voltage V_{oc} is about 10 mV higher, and the short-circuit current density J_{sc} is also higher by about 0·5–0·9 mA/cm^2. These increases contribute to the higher efficiency. Figure 2 shows the absolute external quantum efficiency of the solar cell. The reflectance of the cell measured with a spectrophotometer is also shown. This includes a contribution from the metal grid fingers, and is estimated to be about 2–4% across the entire spectral range. The quantum efficiency rises to a high value just above the CdS absorption edge and remains high in the visible range. The reflectance of the cell rises near the band edge of the absorber, and this is due to the reflectance of the ZnO layer. When this is taken into account, it is clear that the collection efficiency in the red region is also higher than that shown by the external QE curve. This result implies that the diffusion length must be high enough to collect the carriers generated deep in the absorber.

Next, we describe the properties of the absorber material. A thin section of the absorber directly below the cell area was isolated, and material characterization was performed on this slice of as-grown absorber. Figures 3 and 4 show the plan view and cross-sectional images obtained by scanning electron microscopy (SEM). A compact grain structure is observed in cross-section, and faceted grains are visible in plan view. These characteristics are typical of the high-efficiency absorbers grown by the three-stage process. The compositions of the various elements were analyzed by Auger electron spectroscopy, and the profiles are shown in Figure 5 as a function of depth into the absorber. The Ga concentration in the bulk of the sample shows a gradient, which is due to the diffusion properties of Ga during the second stage of the growth. The Ga and In concentrations exhibit variations in the front part, and this is illustrated in a plot of Ga/(Ga + In) ratio shown on the right

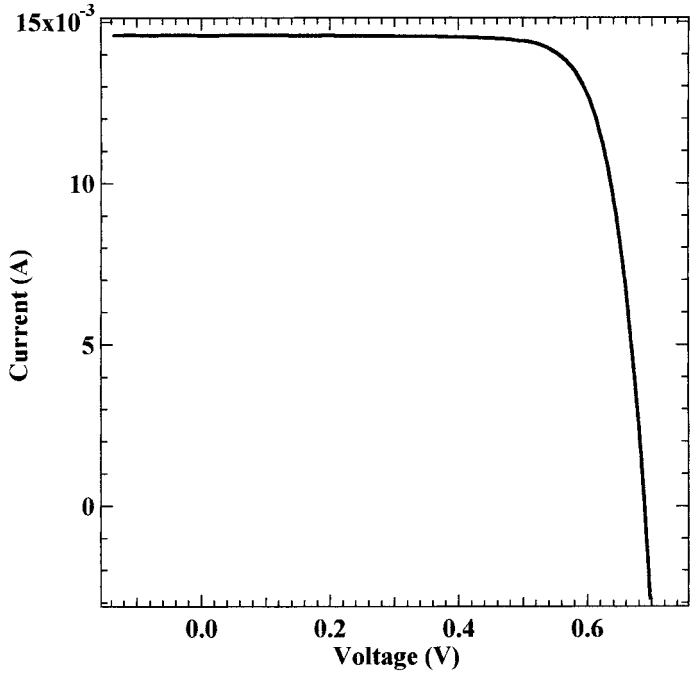

Figure 1. Current–voltage characteristics of the 19·2% efficiency ZnO/CdS/CIGS solar cell. Measured under 1000 W/m^2, AM 1·5 global spectrum at 25°C. Total area of the device is 0·408 cm^2

ordinate. This gradient is related to the ratio of In to Ga in the third stage, the sticking coefficients of In and Ga, and the diffusivity of Ga at the growth temperature. The slopes of these gradients will depend on the growth temperature, the extent to which the local concentration of Cu varies along the substrate, and the amount of Ga in the flux during the third stage. In the present case, the Ga/III ratio exhibits a 'notch', and this gives rise to bandgap grading. The beneficial effect of such grading has been addressed in a prior experimental study.[5] A recent study by Lundberg *et al*.[6] shows that the bandgap grading can increase the V_{oc} by 20–30 mV.

CONCLUSIONS

We have summarized the properties of the highest-efficiency ZnO/CdS/CIGS thin-film solar cells and absorber materials. The new record efficiency of 19·2% is due to the higher V_{oc} and higher J_{sc}, and the potential causes for these improvements are identified. Further work on the effect of bandgap grading, microstructure and defects, and grain boundary passivation can help our knowledge of the device. Greater improvements in current collection can be achieved by using thinner CdS window layers, a wider bandgap alternative, or by completely eliminating the window layer.

Table I. Solar cell parameters for three 19% ZnO/CdS/CIGS cells

Sample	Device	V_{oc} (V)	J_{sc} (mA/cm^2)	Fill factor (%)	Efficiency (%)	Remarks
S2051A1	1	0·689	35·71	78·12	19·2	New record
	2	0·685	35·68	77·91	19·1	
	3	0·680	36·11	77·64	19·1	
C1068-2		0·678	35·22	78·65	18·8	Previous record

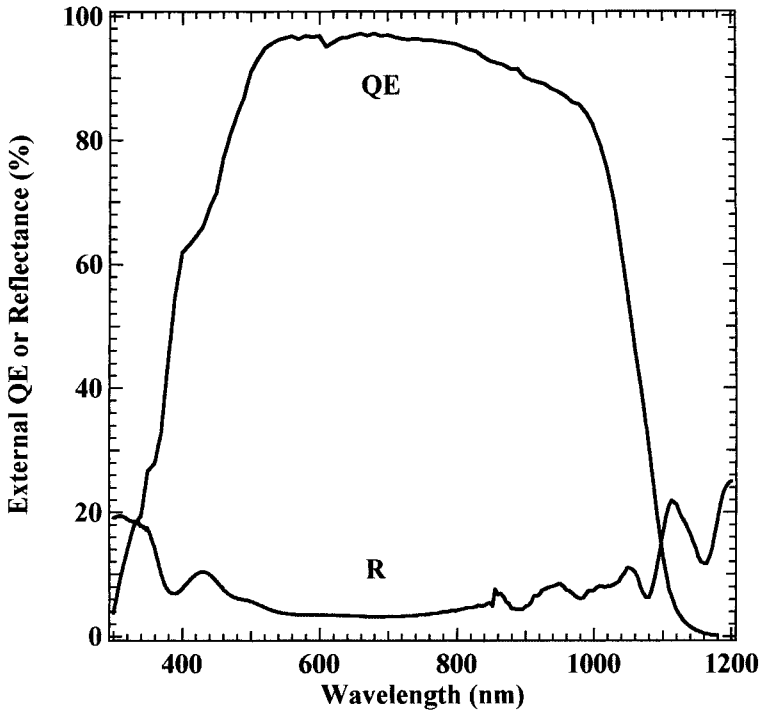

Figure 2. External quantum efficiency and reflectance spectra of the ZnO/CdS/CIGS solar cell

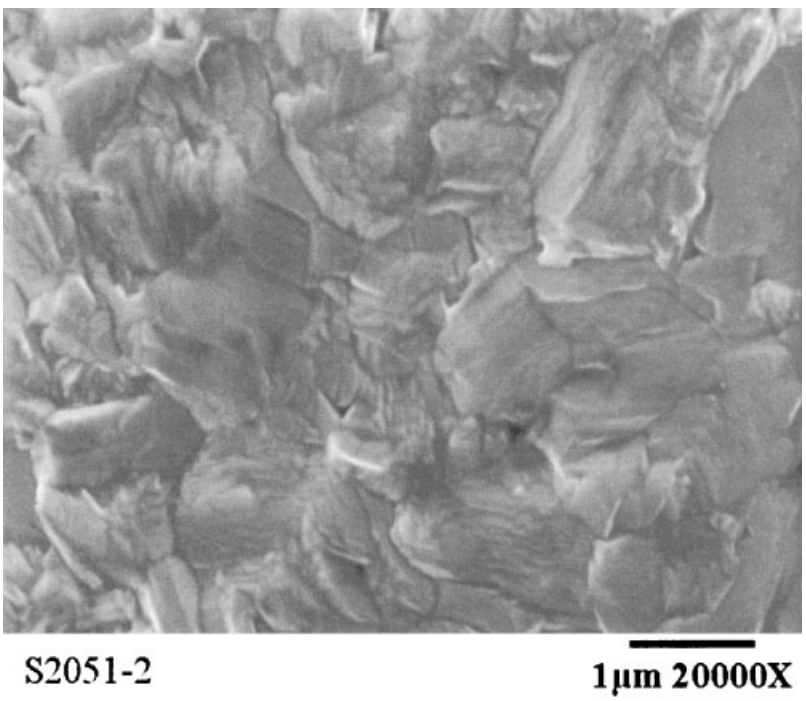

Figure 3. Plan view SEM image of the CIGS absorber

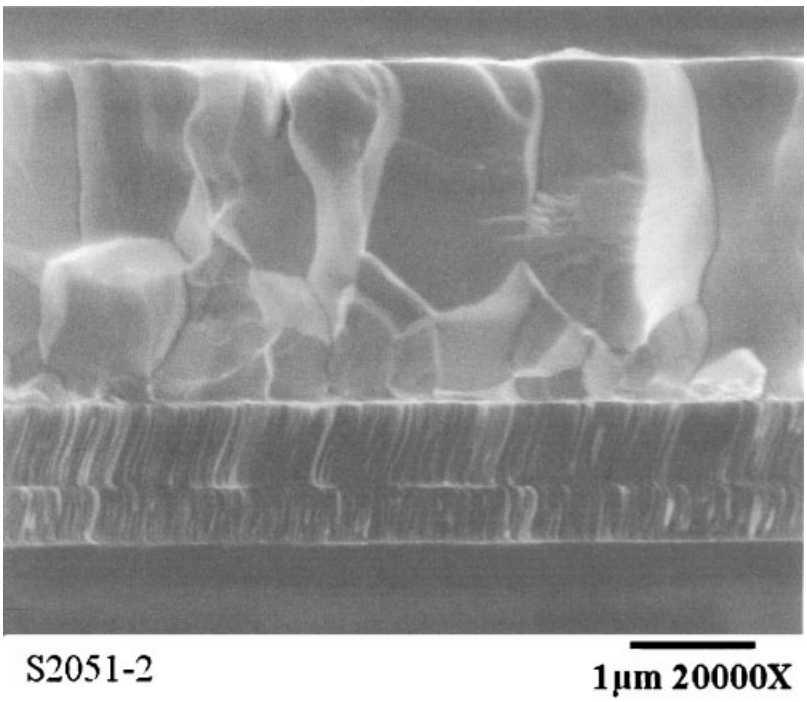

Figure 4. SEM image from a cleaved cross-section of the CIGS absorber

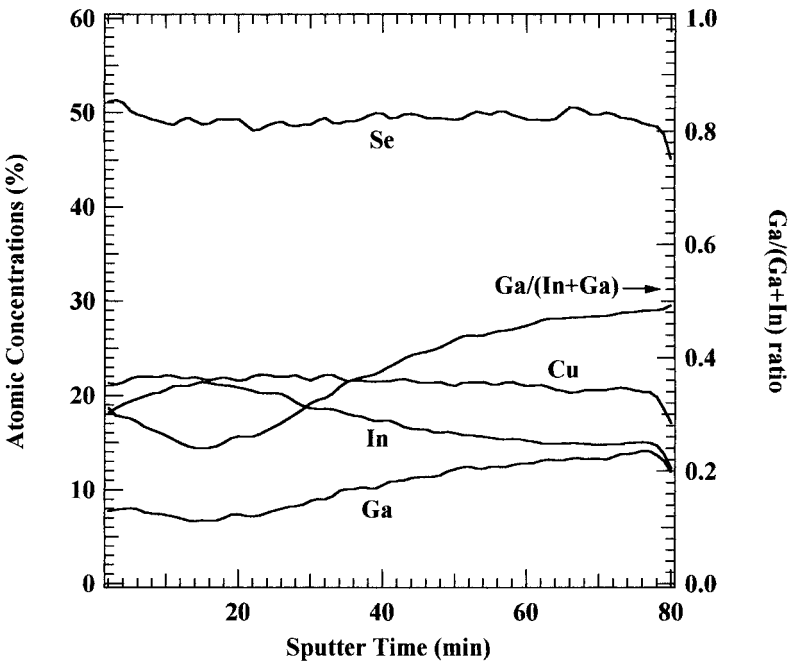

Figure 5. Auger electron spectroscopy profiles of elemental concentrations as a function of depth into the CIGS absorber. The right ordinate shows the calculated Ga/(In + Ga) ratio

Acknowledgements

This work was performed for the USDOE PV Program under Contract DE-AC36-99GO10337 to NREL. The authors would like to thank J. Dolan and J. Alleman for technical assistance; D. Dunlavy, T. Moriarty and K. Emery for cell characterization; and J. Benner and L. L. Kazmerski for their interest and support.

REFERENCES

1. Contreras MA, Egaas B, Ramanathan K, Hiltner J, Swartzlander A, Hasoon F, Noufi R. Progress toward 20% efficiency in Cu(In,Ga)Se_2 polycrystalline thin-film solar cells. *Progress in Photovoltaics: Research and Applications* 1999; **7**: 311–316.
2. Ullal HS, Zweibel K, von Roedern BG. Polycrystalline thin-film photovoltaic technologies: from the laboratory to commercialization. *Proceedings of the 28th IEEE Photovoltaic Specialists' Conference*, Anchorage, 2000; 418–423.
3. Ramanathan K, Wiesner H, Asher S, Niles D, Bhattacharya R, Keane J, Contreras MA, Noufi R. High efficiency thin film solar cells without intermediate buffer layers. *Proceedings of the 2nd World Conference on Photovoltaic Energy Conversion*, Vienna, 1998; 477–481.
4. Satoh T, Hayashi S, Nishiwaki S, Shimakawa S, Hashimoto Y, Negami T, Uenoyama T. Fabrication of Cu(In,Ga)Se_2 by in-line evaporation. *Solar Energy Materials and Solar Cells* 2001; **67**: 203.
5. Gabor AM, Tuttle JR, Swartzlander A, Tennant AL, Contreras MA, Noufi R. Bandgap engineering in Cu(In,Ga)Se_2 thin film solar cells grown from $(In,Ga)_2Se_3$ precursors. *Proceedings of the 1st World Conference on Photovoltaic Energy Conversion*, Hawaii, 1994; 83–86.
6. Lundberg O, Bodegard M, Malmstrom J, Stolt L. Influence of the Cu(In,Ga)Se_2 thickness and Ga grading on solar cell performance. *Progress in Photovoltaics: Research and Applications* 2003; **11**: 77–88.